NBSIR 83-2730

On the Significance of A Wall Effect in Enclosures With Growing Fires

U.S. DEPARTMENT OF COMMERCE
National Bureau of Standards
National Engineering Laboratory
Center for Fire Research
Washington, DC 20234

June 1983

U.S. DEPARTMENT OF COMMERCE
NATIONAL BUREAU OF STANDARDS

NBSIR 83-2730

ON THE SIGNIFICANCE OF A WALL EFFECT IN ENCLOSURES WITH GROWING FIRES

Leonard Y. Cooper

U.S. DEPARTMENT OF COMMERCE
National Bureau of Standards
National Engineering Laboratory
Center for Fire Research
Washington, DC 20234

June 1983

U.S. DEPARTMENT OF COMMERCE, Malcolm Baldrige, *Secretary*
NATIONAL BUREAU OF STANDARDS, Ernest Ambler, *Director*

TABLE OF CONTENTS

LIST OF FIGURES

LIST OF TABLES

ON THE SIGNIFICANCE OF A WALL EFFECT IN ENCLOSURES WITH GROWING FIRES

Leonard Y. Cooper

Abstract

This paper studies the significance of a wall effect that has been observed during the growth stage of enclosure fires. Relative to the two-layer phenomenon which tends to develop during such fires, the effect has to do with the near-wall downward injection of hot upper layer gases into the relatively cool uncontaminated lower layer. It is conjectured that these observed wall flows are buoyancy driven, and that they develop because of the relatively cool temperatures of the upper wall whose surfaces are in contact with the hot upper layer gases. For a growing fire (growth proportional to t^m; t being time and $m \geq 0$) in an enclosed compartment, an analysis of the conjectured mechanism for the wall flow leads to a time-dependent solution for the ratio of wall flow mass ejection rate <u>from</u> the upper layer, $\dot{m}_w$, to the fire plume mass injection rate <u>to</u> the upper layer, $\dot{m}_p$. The solution indicates that in practical fire scenarios $\dot{m}_w/\dot{m}_p$ can be of the order of "several tenths" even prior to the time that the upper layer interface has dropped to an elevation midway between the ceiling and fire. In other words, the results of the analysis indicate the importance of taking the wall effect into account in two-layer zonal analyses of enclosure fire phenomena.

1. INTRODUCTION

The zone approach to mathematical modeling has received much attention in the analysis of enclosure fire environments. In recent years several such zone models have been developed to predict environments in rooms of fire origin as well as in single and even multiple adjacent spaces. Because of the fact that they have each tended to be developed for specific purposes and classes of problems, there is quite a variation from model to model in the amount of attention and detail paid to the simulation of different physical phenomena that come into play. In this regard, however, even the most sophisticated of the models have tacitly ignored a commonly observed and potentially important wall effect which can lead to significant features of enclosure fire environments not heretofore simulated.

After describing the wall effect in question this paper will then identify the conditions under which the effect is significant. Finally, the paper will propose a general purpose algorithm for including the wall effect in an overall zonal model analysis.

2. A DESCRIPTION OF THE WALL EFFECT AND A MEASURE OF ITS SIGNIFICANCE

The wall effect under consideration is first described and analyzed within the context of a generic fire scenario which develops within an enclosure lacking any significant ventilation openings (any leakage from the enclosure is assumed to occur near the floor). Later, the relation of the wall effect to fire environments developing in enclosures with open doors or windows will be addressed.

A sketch of the significant features of all the conjectured wall effects to be described below is presented in figure 1.

A fire starts a distance H below the ceiling of an enclosure of floor area, A, and releases energy at the rate Q(t), where t is time from the effective instant of ignition. Because of their elevated temperature, the products of combustion from the fire are driven upwards by buoyancy forces, and a turbulent plume is generated. All along the axis of the plume, quiescent ambient air is entrained laterally into and mixed with the plume gases. The plume eventually impinges on the ceiling and spreads radially outward along this surface forming a relatively thin, turbulent ceiling jet. The ceiling jet gases redistribute themselves across the entire ceiling area of the enclosure, start to fill the upper enclosure volume, and eventually submerge all the continuous ceiling jet flow activity. Below this jet activity the now reduced momentum plume gases form a relatively quiescent, elevated temperature, upper gas layer which continues to increase in depth as the plume gas upward filling process continues in time. The elevation above the fire of the lower interface of this gas layer is designated by $Z_i(t)$.

Except for regions near the bounding ceiling and wall surfaces, it is reasonable to characterize the upper layer as being uniform in composition with an absolute temperature, $T_u(t)$ and with concentrations of products of combustion i, $C_i(t)$ (units of product per unit mass of bulk upper layer mixture).

The ceiling surface temperatures are generally different from T_u. This surface is heated from the initial ambient temperature, T_∞, by convection from the high temperature ceiling jet gases and by radiation from the fire's combustion zone. Later into the fire, radiation exchanges from the bulk upper layer gases at T_u and from other bounding surfaces of the enclosure may also become significant.

In general the temperatures of the wall surfaces are also different from T_u. The radiant heating mechanism of these surfaces is similar to that for the ceiling. However, except for possible locations of strong ceiling jet-wall surface flow interactions (i.e., where wall surfaces are close enough to the plume-ceiling impingement point), the vigorous convective heat transfer at the ceiling is generally absent at the walls. Thus, one can anticipate that the wall surfaces will be heated from the initial temperature, T_∞, at a significantly lower rate than the ceiling surface.

It is conjectured and seems to have been observed[1,2] that the condition of relatively cool walls, at absolute temperature, T_w, bounding the elevated temperature upper layer gases, at T_u, would lead to the development of a classic, two-dimensional, downward-directed, natural convection or buoyancy-driven boundary layer flow along the upper portion of the vertical wall surfaces. The phenomenon would occur in this basic form away from locations of vigorous ceiling jet-wall interactions. The boundary layer flow would originate near the ceiling, increase in mass and momentum flux with decreasing elevation, and, at the upper layer - lower layer interface, be injected into the lower layer of the enclosure as a downward-directed wall jet of upper layer gases. The injected gases would have a bulk temperature lower than the upper-layer gases but higher than the relatively cool and uncontaminated lower-layer gases.

Once in the lower layer, the downward-directed wall jet of the now upwardly-buoyant, product of combustion laden gas would be buoyed back upward and away from the wall to either mix with and contaminate the lower layer air or to entrain additional (i.e., in addition to the fire plume) lower layer air into the upper layer.

Whatever the eventual disposition of the wall flow contaminents, the basic wall flow phenomenon could significantly alter the rate of development of life-threatening conditions in the enclosure. If, for example, the flow is buoyed upward as a wall plume and re-enters the upper layer, then, having entrained additional lower layer air, the depth of the upper layer will grow more rapidly than it would have otherwise, albeit at a reduced temperature and product concentration. On the other hand, if the wall flow is mixed with the lower layer gas, then the net effect would be a contamination of the lower layer, less rapid growth in upper layer depth and at increased temperature and concentration.

When the mass flux leaving the upper layer in the wall flow is large enough to significantly retard the velocity of descent, dZ_i/dt, of the upper layer - lower layer interface or to lead to significant increases in temperature and/or product of combustion contamination of the lower layer, then this flow must be taken account of in a mathematical simulation of the overall enclosure environment.

Let $\dot{m}_p$ be the mass flux of the plume into the upper layer, i.e., at Z_i. Also, let $\dot{m}_w$ be the total mass flux of the wall boundary layer flow ejected at Z_i from the upper layer. Then, consistent with the above, an analysis of the enclosure environment which does not include an accounting of the wall flows can lead to reliable results only when $\dot{m}_w << \dot{m}_p$. Thus when $\dot{m}_w/\dot{m}_p << 1$ the wall effect can be neglected, and when this is not the case it must be taken into account. This will be referred to below as the Wall Effect Criterion.

It is noteworthy that the described wall flow phenomenon would not necessarily occur only in rooms of fire origin. Indeed, it can also play an important role in the redistribution of the products of combustion in spaces which are adjacent to, or communicate with rooms-of-fire-origin. Here, the fire generated plume in the above room-of-fire-origin scenario would be replaced, for example, by an analogous upper doorway plume which was generated by inflowing combustion products. "Smoke layering" in the adjacent space would be initiated in the usual way. Also, at least until relatively late into the fire when radiative heating of adjacent space wall surfaces could become substantial, these surfaces, being only weakly heated by the conjectured buoyancy driven wall flows, would likely remain close to their original ambient temperature.

The above discussion is from the perspective of the early growth stage of the fire when a definitive $(T_u - T_w)$ temperature differential exists, when no significant differential between the lower wall temperature and the lower gas temperature, T_L, (both of which are initially at T_∞) has developed, and when the overall wall flow activity, as described earlier, is conjectured to occur. As time moves on, however, a substantial difference between T_L and the (probably) relatively greater lower wall temperature (heated primarily by radiation) may begin to develop. At least near the floor of the enclosure this would (probably) tend to lead to an upward-directed, lower wall flow. It is also possible that such a lower wall flow would become relatively strong at a time when the downward-directed, upper wall flow starts to decrease in strength by virtue of a reduction in $(T_u - T_w)$. Under such a circumstance, the nature of the interaction of such combined, counter-current wall flows could be important in an adequate description of the overall enclosure environment; the early growth stage description of a dominant upper wall flow would have to be revised.

An analysis of the combined wall flow effect, which may come into play at later stages of the fire, is outside the intended scope of the present paper. The combined flow effect will not be discussed further except to note that a study has been recently initiated on the significance of the phenomenon in ventilated enclosure fire scenarios during steady state conditions.[3]

3. SOME PROPERTIES OF THE WALL FLOW

Refering to the wall flow depicted in figure 1, the total mass flux, $\dot{m}(x)$, at a distance $x = H - Z$ below the ceiling (Z above the fire) can be estimated, for Prandtl Number (Pr) = 0.72 and according to whether the boundary layer is laminar or mostly turbulent, from

$$\frac{\dot{m}(x)}{P} = \begin{cases} 1.70\ \mu_\infty Gr_x^{1/4}; & \text{Laminar}: Gr_x < 0.5(10^9) \\ 0.102\ \mu_\infty Gr_x^{2/5}; & \text{Turbulent}: Gr_x > 1.5(10^{10}) \end{cases} \tag{1}$$

where P is the total length of the perimeter of the enclosure, Gr_x is the Grashoff number

$$Gr_x = \frac{(T_u - T_w)gx^3}{T_\infty \nu_\infty^2} = (\phi_u - \phi_w)(1 - \zeta)^3 \frac{gH^3}{\nu_\infty^2} \tag{2}$$

and where dimensionless values of T_u, T_w, and Z have been defined as

$$\phi_u = T_u/T_\infty; \; \phi_w = T_w/T_\infty; \; \zeta = Z/H \tag{3}$$

The above estimates for $\dot{m}(x)$ were established from results presented in references 4-6. The Gr_x bounds for a laminar or mostly turbulent boundary layer are from reference 7. The Bousinesq approximation was used in developing eq. (1), and will be used throughout the analysis to follow. All gas properties will be taken as those of air at standard ambient conditions. The wall temperature is taken to be uniform.

From the origin of the boundary layer to some x above the interface ($0 < x < H - Z_i$), the average rate of heat transfer per unit area, $\overline{q}''$, to the wall can be estimated from

$$\overline{q}'' = \overline{h}\,(T_u - T_w) \tag{4}$$

where

Average Nusselt Number =

$$\overline{Nu}_x = \frac{x\overline{h}}{k} = \begin{cases} 0.48\, Gr_x^{1/4}, \text{ Laminar}^5 \\ 0.0184\, Gr_x^{2/5}, \text{ Turbulent}^6 \end{cases} \tag{5}$$

and where k is the thermal conductivity of the gas mixture. Below the interface the heat transfer rate will be less than $\overline{q}''$.

The mixing cup temperature, T_m, of the wall flow at position x is defined by

$$T_u - T_m = \frac{\overline{q}'' P x}{\dot{m} C_p} \tag{6}$$

where C_p is the specific heat.

Using Pr = 0.72, the results of eqs. (1), (4) and (5) in eq. (6) lead to the following estimate for T_m:

$$\frac{T_u - T_m}{T_u - T_w} = \begin{cases} 0.39, & \text{Laminar} \\ 0.25, & \text{Turbulent} \end{cases} \tag{7}$$

This last result indicates that T_m is independent of x and somewhat closer to T_u than to T_w. In particular, eq. (7) is valid at the interface position $x = x_i = H - Z_i$.

The kinematic momentum flux, K, of the wall flow

$$K = \int_0^\infty u^2 dy \tag{8}$$

where u is the downward velocity and y is the distance from the wall surface, can be estimated from results of integral boundary layer analyses in references 6 and 7. Thus, for Pr = 0.72

$$K = \begin{cases} 2.25\nu_\infty^2 \, Gr_x^{3/4}/x, \text{ Laminar} \\ 0.0366\nu_\infty^2 \, Gr_x^{9/10}/x, \text{ Turbulent} \end{cases} \tag{9}$$

Finally, the order of magnitude of the downward velocity will be of interest in later discussion. From results in references 4 and 6 it is possible to obtain the result that for $Pr = 0.72$ the maximum velocity in the boundary layer, u_{max}, for both laminar and mostly turbulent flow can be estimated from

$$u_{max} = 0.55\nu_\infty \, Gr_x^{1/2}/x \tag{10}$$

4. IMPLICATIONS OF THE WALL EFFECT CRITERION

The mass flux of the plume at the upper layer - lower layer interface can be estimated from[8,9]

$$\dot{m}_p = 0.21\rho_\infty g^{1/2} H^{5/2} (1 - \lambda_r)^{1/3} Q_o^{*1/3} \zeta_i^{5/3} \psi^{1/3} \tag{11}$$

where

$$\zeta_i = Z_i/H, \ \psi = Q(t)/Q_o, \ Q_o^* = \frac{Q_o}{\rho_\infty C_p T_\infty g^{1/2} H^{5/2}} \tag{12}$$

and where Q_o is a characteristic energy release rate, and $(1 - \lambda_r)$ is the fraction of Q which effectively acts to heat the plume gases and ultimately drive the plume's upward momentum. λ_r is approximately the fraction of Q lost by radiation from the combustion zone and plume. For hazardous flaming fires, λ_r is typically in the range 0.3 - 0.4.[8] In real fires, the simple description of Eq. (11) has been shown to yield excellent results above the combustion zone when the "point" location is taken to be at the lowest elevation of the combustion zone or plume above it where "free unrestricted", lateral entrainment of ambient air is possible.[8,10,11]

In order to invoke the Wall Effect Criterion, eqs. (1) and (11) are used to estimate $\dot{m}_w/\dot{m}_p$ with the result

$$\dot{m}_w/\dot{m}_p = \frac{\alpha Gr^n (P/H)}{0.21(1-\lambda_r)^{1/3} Q_o^{*1/3} \zeta_i^{5/3} (gH^3/\nu_\infty^2)^{1/2} \psi^{1/3}} \tag{13}$$

where

$$Gr = Gr_x(x = x_i = H-Z_i) = (\phi_u - 1)(1-\delta)(1-\zeta_i)^3 gH^3/\nu_\infty^2 \tag{14}$$

$$\delta = (\phi_w - 1)/(\phi_u - 1) \tag{15}$$

$$\begin{aligned} &\alpha = 1.70,\ n = 1/4 \text{ if } Gr < 0.5(10^9), \text{ Laminar} \\ &\alpha = 0.102,\ n = 2/5 \text{ if } Gr > 1.5(10^{10}), \text{ Turbulent} \end{aligned} \tag{16}$$

To apply eq. (13) to the dynamic fire scenario discussed in the last section it is now necessary to estimate the values of $\zeta_i(t)$, $\phi_u(t)$ and $\phi_w(t)$.

In the absence of any wall effect, and from ignition ($\zeta_i = 1$) up to the time that the interface elevation starts to approach the elevation of the fire (i.e., ζ_i becomes small), the solutions for $\zeta_i(t)$ and $\phi_u(t)$ have been previously obtained[10] for enclosure fires where $Q(t) \sim t^m$ (arbitrary $m \geq 0$), and where any pressure relieving leakage from the enclosure is primarily near the lower portions of the enclosure boundary. Under such circumstances

$$\phi_u = \{1-(m + 3)\varepsilon\tau^{3(m+1)/(m+3)}/[3(m+1)(1-\zeta_i)]\}^{-1} \tag{17}$$

where

$$\varepsilon = (1-\lambda_c)\{[(m+3)/3]^m Q_o^*\}^{2/(m+3)}/(1-\lambda_r)^{(m+1)/(m+3)} \tag{18}$$

$$\tau = 3[(1-\lambda_r)Q_o^*]^{1/3}(tH^{3/2}g^{1/2}/A)^{(m+3)/3}/(m+3) \tag{19}$$

and where Q_o is explicitly defined as

$$Q_o = (Q/t^m)(H^{3/2}g^{1/2}/A)^{-m} \tag{20}$$

Also, λ_c is defined as the fraction of Q which is instantaneously transfered to the internal bounding surfaces of the enclosure. $\lambda_c Q$ would include all heat transfer to surfaces by both convection and radiation, and λ_c is typically in the range[9] 0.6 - 0.9. For magnitudes of energy release rates and enclosure sizes of practical interest[12], $\varepsilon << 1$ and ζ_i can be estimated from

$$\lim_{\varepsilon \to 0} \zeta_i = (1 + 0.140\tau)^{-3/2}[1 + O(\varepsilon)] \tag{21}$$

for ζ_i and m which include the ranges $0.5 \leq \zeta_i \leq 1$ and $0 \leq m \leq 2$. (For a more definite idea of the utility of the eq. (21) approximation refer to figure 2 of reference 12.) Unless noted otherwise all further estimates in this paper will only be applicable when the above approximation yields an acceptable estimate for $\zeta_i(\tau)$.

Using eqs. (17) and (21), and eliminating the explicit dependence of ϕ_u on time leads to

$$\lim_{\varepsilon\to 0} (\phi_u - 1) = \frac{\varepsilon(m+3)}{3(m+1)(1-\zeta_i)} \left(\frac{\zeta_i^{-2/3}-1}{0.140}\right)^{3(m+1)/(m+3)} + O(\varepsilon)^2 \tag{22}$$

Using eq. (22) in eq. (14) and rewriting eq. (13) eventually leads to

$$\dot{m}_w/\dot{m}_p \approx \frac{\alpha Gr^n X_2}{0.21 X_1^{1/2} \zeta_i^{5/3}} \left(\frac{0.140}{\zeta_i^{-2/3} - 1}\right)^{\frac{m}{(m+3)}} \tag{23}$$

$$\begin{aligned} Gr &= Gr(\zeta_i;\ X_1,\ m,\ \delta) \\ &\approx \frac{(1-\delta)(m+3)}{3(m+1)} X_1 (1-\zeta_i)^2 \left(\frac{\zeta_i^{-2/3}-1}{0.140}\right)^{\frac{3(m+1)}{(m+3)}} \end{aligned} \tag{24}$$

where α and n are given in eq. (16), and where X_1 and X_2 are defined according to

$$X_1 = \frac{g\varepsilon H^3}{\nu_\infty^2}\ ;\ X_2 = \left(\frac{1-\lambda_c}{1-\lambda_r}\right)^{1/2} \left(\frac{P}{H}\right) \tag{25}$$

4.1 Applying Results When Wall Temperatures Are Close to Ambient

During the early growth stage of the fire the increase of T_w above its initial value, T_∞, will often develop at a much slower rate than will the increase of T_u. Thus, for the purpose of evaluating the significance of the wall effect, it is reasonable to investigate the implications of eqs. (23) and (24) under the condition

$$\delta << 1 \tag{26}$$

According to these equations, and for m = 0, 1.0, and 2.0, figure 2 presents plots of ζ_i as a function of X_1 with $(\dot{m}_w/\dot{m}_p)/X_2$ as a parameter, under the condition $\delta = 0$. Thus, for $0 \leq m < 2.0$, and for a specified X_1 fire scenario, the plots of figure 2 can be used to determine the value of ζ_i below which the wall effect starts to become significant (i.e., $\dot{m}_w/\dot{m}_p$ becomes larger than, say, several tenths).

The results of figure 2 will be used to evaluate the significance of the wall effect during test runs of two full-scale enclosure fire test programs reported in references 1 and 2. As mentioned earlier, the wall effect seems to have played a role in those experiments.

The first evaluation refers to a constant 16.2 kW enclosure fire reported in reference 2. The fire was an acetylene diffusion flame generated from a gas burner source 2.06 m below the ceiling and in the center of a square, "fully" enclosed space (designed to leak from below) with sides of length 3.64 m. Tests on the burner indicated a 50% radiation loss from the sooty flame ($\lambda_r = 0.5$). Total loss to the ceiling and walls was estimated to be 84% ($\lambda_c = 0.84$). In terms of previous definitions, and using the values $T_\infty = 294^0K$, $\rho_\infty = 1.2\ kg/m^3$, $\nu_\infty = 1.5\ (10^{-5})\ m^2/s$, $C_p = 240\ cal/(kg°K)$, and $g = 9.8\ m/s^2$ here and in all later calculations, the test run is found to be characterized by

$$m = 0,\ \varepsilon = 0.0036,\ X_1 = 1.4(10^9),\ X_2 = 4.0$$

Now assume the wall effect to be significant when $\dot{m}_w/\dot{m}_p > 0.3$, i.e., $(\dot{m}_w/\dot{m}_p)/X_2 > 0.075$. Then figure 2 for m=0 leads to the conclusion that the wall effect must be taken account of once ζ_i drops to 0.62, i.e., once the upper layer thickness exceeds 0.78 m.

The remaining evaluations will refer to test runs reported in reference 1 in a 2.36 m high, fully enclosed two to three room space (designed to leak from below), where one of the rooms, having an area of 14.0 m^2 and designated as the burn room, contained a centrally located methane burner 2.12 m below the ceiling. The one to two rooms adjacent to the burn room were corridor-like in configuration, and the total multi-room test space area ranged from 40.6 - 89.6 m^2. For test runs with all rooms freely connected (i.e., full open doorways), data indicated that after an initial time interval a single room, two layer mod had some applicability in analyzing the dynamic conditions within the overall space. It is therefore reasonable to utilize the present room-of-fire-origin results in an evaluation of the significance of the wall effect under consideration. As mentioned earlier, the existence of the wall effect was observed during the course of both the reference 1 and reference 2 test programs.

The first evaluation of the above test series will involve the smallest constant fire, 25 kW, and the largest test space area, 89.6 m^2 of the test program. This configuration had a total wall perimeter of approximately 81 m. Previous tests on the burner had indicated $\lambda_r = 0.19$, and data from vertical arrays of thermocouples indicated an average value $\lambda_c = 0.87$. Using all of the above data the test run is found to be characterized by

$$m = 0,\ \varepsilon = 0.0032,\ X_1 = 1.3(10^9),\ X_2 = 15.$$

Again, assuming the wall effect to be significant when $\dot{m}_w/\dot{m}_p > 0.3$, i.e., $(\dot{m}_w/\dot{m}_p)/X_2 > 0.020$, figure 2 leads to the conclusion that the wall effect must be taken account of once ζ_i drops to 0.85, i.e., once the upper layer thickness exceeds 0.32 m.

The second evaluation of the test series will involve the largest constant fire, 225 kW, and the smallest test space area, 40.6 m^2, of the test program. This configuration had a total wall perimeter of approximately 43 m. Tests on the burner indicated $\lambda_r = 0.24$ for burner fires in the range 50 to several hundred kW, and test run data indicate an average value $\lambda_c = 0.75$. All of this leads to

$$m = 0,\ \varepsilon = 0.027,\ X_1 = 1.1(10^{10}),\ X_2 = 12.$$

Using the previous criterion and figure 2, the wall effect is predicted to be significant here once $\zeta_i < 0.76$.

The final two test run evaluations will refer to the largest and smallest area configurations where the burner was controlled to generate a fire growing linearly with time according to

$$Q(t) = (t/2)\ \text{kW/s} \tag{27}$$

Thus, m = 1, and according to eq. (20)

$$Q_o = [A/(2H^{3/2}g^{1/2})] \text{ kW/s} \tag{28}$$

First the largest space ($A = 89.6$ m^2, $P = 81$ m): Here $\lambda_r = 0.24$, and test data indicate an average value $\lambda_c = 0.81$. This leads to

$$m = 1,\ \varepsilon = 0.0064,\ X_1 = 2.6(10^9),\ X_2 = 39.$$

Using the previous criterion and the $m = 1.0$ plots of figure 2, the wall effect is predicted to be significant once $\zeta_i < 0.93$.

Finally, the smallest space ($A = 40.6$ m^2, $P = 43$ m): Here $\lambda = 0.24$, and test data indicate an average value $\lambda_c = 0.71$. This leads to

$$m = 1,\ \varepsilon = 0.0065,\ X_1 = 2.7(10^9),\ X_2 = 27.$$

From figure 2, the wall effect is predicted to be significant once $\zeta_i < 0.90$.

5. ESTIMATING THE WALL TEMPERATURE

Figure 2 and the above example calculations were based on the assumption $\delta << 1$ of eq. (26). In this section estimates of δ will be developed so that the validity of this assumption can be evaluated, and so that, when required, estimates of $\dot{m}_w/\dot{m}_p$ under somewhat more general nonambient wall temperature conditions can be obtained from eqs. (23) and (24).

In order to predict δ, estimates for $\phi_w - 1$ under each of two different wall heating conditions will be established; increases of $\phi_w - 1$ due to possible radiation from the fire's combustion zone, and increases of $\phi_w - 1$ at the upper wall surfaces due to convective heating from the wall layer flows. For the purpose of this investigation it is assumed that for the fire's growth stage of present interest, and far enough away from significant ceiling jet - wall flow interaction, one of these two mechanisms will dominate the increase of ϕ_w.

5.1 Wall Heating Due to Radiation

Increases in ϕ_w due to radiation may be the more significant of the heating mechanisms for enclosure spaces which are configured in such a manner that a large fraction of the total wall surface is illuminated by the fire's combustion zone. Under such circumstances and for the purpose of estimating $\phi_w - 1$ and comparing it to $\phi_u - 1$, assume the fire to be a characteristic distance $(A/\pi)^{1/2}$ from all wall surfaces. Then the average rate of wall heat transfer due to radiation from the combustion zone, q''_R, can be estimated by

$$q''_R = \frac{\lambda_r Q(t)}{4A} \tag{29}$$

For the purpose of the present estimate, first consider wall materials which are thermally thick up to some time, t_I, of interest. To be definite, it is reasonable to consider a wall material as thermally thick if its thickness, L_{THICK}, and thermal diffusivity, κ_w, satisfy

$$L_{THICK} > 2\sqrt{\kappa_w t_I} \tag{30}$$

For t_I of 3 minutes, and using material properties from table 1, the criterion would be satisfied, for example, with gypsum board walls thicker than 0.011 m or concrete walls thicker than 0.055 m.

Using the thick wall assumption and eq. (29) in Carslaw and Jaeger's solution[13] to the appropriate, specified flux, heat conduction problem for the wall leads to the result

$$\phi_w - 1 = \frac{\lambda_r K_w^{1/2} Q_o}{4T_\infty \pi^{1/2} A k_w} \int_0^t \frac{\psi(t-\eta)}{\eta^{1/2}} d\eta \qquad (31)$$

where k_w is the thermal conductivity of the wall material.

For the t^m fire growth studied earlier, eq. (31) can be integrated to yield

Radiation to Thermally Thick Wall:

$$\phi_w - 1 = 0.14 X_3 X_1^{1/4} \frac{\varepsilon(m+3)^{1/2}\Gamma(m+1)}{\Gamma(m+1/2)} \left(\frac{\zeta_i^{-2/3}-1}{0.140}\right)^{\frac{3(2m+1)}{2(m+3)}} \qquad (32)$$

$$\delta = 0.43 X_3 X_1^{1/4} \frac{(m+1)^{1/2}\Gamma(m+1)}{\Gamma(m+1/2)} (1-\zeta_i) \left(\frac{0.140}{\zeta_i^{-2/3}-1}\right)^{\frac{3}{2(m+3)}} \qquad (33)$$

where

$$X_3 = \frac{\lambda_r}{(1-\lambda_r)} \left(\frac{1-\lambda_r}{1-\lambda_c}\right)^{5/4} \left(\frac{\kappa_w}{\kappa}\right)^{1/2} \left(\frac{k}{\kappa_w}\right) \frac{Pr^{1/2} H}{A^{1/2}} \qquad (34)$$

$\Gamma(x)$ is the Gamma function, X_1 is defined in eq. (25), and κ and k are the thermal diffusivity and conductivity of air at ambient conditions.

The above result can now be applied to the previously discussed 16.2 kW enclosure fire (gypsum board wall) of reference 2. The geometry of fire scenario is one where all walls of the enclosure are illuminated by the fire, and where radiation can be anticipated to dominate the wall surface heating. Using the previously identified parameters of that fire, and the κ, k values of table 1 in eq. (33) leads to

$$\delta = (\phi_w - 1)/(\phi_u - 1) = 0.29 \text{ at } \zeta_i = 0.62$$

Note that this ratio is small enough to allow the $\delta = 0$ estimate of figure 2 to be useful. Indeed, if the approximation of eq. (26) is supplanted by the newly revised estimate

$$\phi_u - \phi_w = (\phi_u - 1)(1 - \delta) = 0.71(\phi_u - 1)$$

then eqs. (23) and (24) would predict $\dot{m}_w/\dot{m}_p = 0.28$ at $\zeta_i = 0.62$, instead of the earlier estimate of $\dot{m}_w/\dot{m}_p = 0.30$.

If the wall of the reference 2 enclosure had been concrete instead of gypsum board (and if λ_c would not have been significantly different from the measured value of 0.84), then eq. (33) leads to the estimate

$$\delta = (\phi_w - 1)/(\phi_u - 1) = 0.09 \text{ at } \zeta_i = 0.62$$

Besides thermally thick walls, wall temperatures for thermally thin walls are also of interest. Again, for definiteness, it is reasonable to consider a wall material as thermally thin if its thickness L_{THIN} satisfies

$$L_{THIN} < 0.6\sqrt{\kappa_w t_I} \tag{35}$$

Using material properties from reference 11 and a t_I of 3 minutes, this criterion would be satisfied, for example, with mild steel walls thinner than 0.028 m, glass walls (windows) thinner than 0.006 m, or wood panel walls thinner than 0.004 m.

Using the radiant heat transfer rate of eq. (29) and the t^m fire growth leads to

Radiation to Thermally Thin Rear-Insulated Wall:

$$\phi_w - 1 = \frac{\varepsilon}{12} X_4 \left(\frac{m+3}{m+1}\right) \left(\frac{0.140}{\zeta_i^{-2/3} - 1}\right)^{\frac{3(m+1)}{(m+3)}} \tag{36}$$

$$\delta = 0.25\ X_4(1 - \zeta_i) \tag{37}$$

where

$$X_4 = \frac{\lambda_r}{(1 - \lambda_c)} \left(\frac{H}{L_{THIN}}\right) \left(\frac{\kappa_w}{\kappa}\right) \left(\frac{k}{\kappa_w}\right) \tag{38}$$

If the wall of the reference 2 enclosure had been sheet metal construction of thickness 0.0015 m instead of gypsum board (and if λ_c was not significantly different than the measured value of 0.84), then eq. (37) leads to the estimate

$\delta = 0.13$ at $\zeta_i = 0.62$

and the original small δ determination of the significance of the wall effect continues to be relevant.

5.2 Wall Heating Due to Convection

In some enclosure fire configurations, radiant heating of enclosure wall surfaces from the fire's combustion zone may play a relatively minor role compared to convection. This would be the case, for example, if direct, line-of-sight, combustion zone illumination of most wall surfaces was blocked by furniture or segmented partitions, or on account of an alcove-like fire location. Also, in a multi-room enclosure configuration, which is an extension of the alcove-like single room configuration, radiant wall heating in rooms other than the room-of-fire-origin could play a minor role well into the "smoke-filling" process.

An estimate for the convection driven $\phi_w(t)$ increase, to be obtained here, will be based on an eq. (4) heat flux to the wall at every instant of time, t^*, from $t^* = 0$ to $t^* = t$. $\overline{h}(t^*)$ in eq. (4) will be computed from eq. (5) with $x = H - Z_i(t^*)$ and with $Gr_x = Gr(t^*)$ according to eq. (14) or (24). In the estimate, δ will be neglected compared to 1 and a laminar wall layer will be assumed through most of the heating history up to the time, t, of interest.

All of the above considerations lead to a convective wall flux, $\bar{q}''_C$, given by

$$\bar{q}''_C(t^*) = \frac{0.48}{3^{5/4}}\frac{T_\infty}{H}\,k\varepsilon\left(\frac{m+3}{m+1}\right)^{5/4}\frac{X_1^{1/4}}{[1-\zeta_i]^{3/2}}\,\tau^{\frac{15(m+1)}{4(m+3)}} \tag{39}$$

where τ is evaluated from eq. (19) with $t = t^*$. Using this last result in the reference 13 solution to the specified flux heat conduction problem for a thermally thick wall leads to the result

Convection to Thermally Thick Wall:

$$\phi_w - 1 = \frac{0.17\varepsilon X_5}{(1-\zeta_i)^{1/2}}\left(\frac{\zeta_i^{-2/3}-1}{0.14}\right)^{\frac{11m+9}{4(m+3)}} \cdot \frac{(m+3)^{7/4}}{(m+3)^{1/4}}\frac{\Gamma[3(m+1)/4]}{\Gamma[3(m+3)/4]}\frac{I_1(1-\zeta_i;m)}{I_1(0;m)} \tag{40}$$

$$\delta = \frac{0.31X_5(1-\zeta_i)^{1/2}}{(\zeta_i^{-2/3}-1)^{1/4}}\;\frac{(m+3)^{3/4}}{(m+1)^{1/4}}\frac{\Gamma[3(m+1)/4]}{\Gamma[3(m+3)/4]}\frac{I_1(1-\zeta_i;m)}{I_1(0;m)} \tag{41}$$

where

$$X_5 = \left(\frac{1-\lambda_c}{1-\lambda_r}\right)^{1/4}\frac{A^{1/2}}{Pr^{1/2}H}\left(\frac{\kappa_w}{\kappa}\right)^{1/2}\left(\frac{k}{\kappa_w}\right) \tag{42}$$

$$I_1(x;m) = \int_0^1\left[\frac{(1-x\eta)^{-2/3}-1}{(1-x)^{-2/3}-1}\right]^{\frac{11m+15}{4(m+3)}} \cdot \left\{1-\left[\frac{(1-x\eta)^{-2/3}-1}{(1-x)^{-2/3}-1}\right]^{\frac{3}{(m+3)}}\right\}^{1/2}\frac{d\eta}{(1-x\eta)^{5/3}\eta^{3/2}} \tag{43}$$

$$I_1(0;m) = \frac{(m+3)}{3}\frac{\Gamma(3/2)\Gamma[3(m+1)/4]}{\Gamma[3(m+3)/4]} \tag{44}$$

and where $I_1(x;m)/I_1(0;m)$ has been evaluated and plotted in figure 3 for $m = 0$, 1.0, 2.0, and 5.0.

The convective wall flux of eq. (39) has also been used to obtain $\phi_w - 1$ and δ for thermally thin wall constructions, viz

Convection to Thermally Thin Rear-Insulated Wall:

$$\phi_w - 1 = \frac{0.26\varepsilon X_6 X_1^{-1/4}}{(1-\zeta_i)^{1/2}} \left(\frac{\zeta_i^{-2/3}-1}{0.14}\right)^{\frac{11m+15}{4(m+3)}} \cdot \left(\frac{m+3}{m+1}\right)^{9/4} \frac{I_2(1-\zeta_i;m)}{I_2(0;m)} \tag{45}$$

$$\delta = 0.77 X_6 X_1^{-1/4} (1-\zeta_i)^{1/2} \left(\frac{\zeta_i^{-2/3}-1}{0.14}\right)^{-\frac{(m-3)}{4(m+3)}} \cdot \left(\frac{m+3}{m+1}\right)^{5/4} \frac{I_2(1-\zeta_i;m)}{I_2(0;m)} \tag{46}$$

where

$$X_6 = \left(\frac{1-\lambda_c}{1-\lambda_r}\right)^{1/2} \frac{A}{L_{THIN} HPr} \left(\frac{\kappa_w}{\kappa}\right)\left(\frac{k}{\kappa_w}\right) \tag{47}$$

$$I_2(x;m) = \int_0^1 \left[\frac{(1-x\eta)^{-2/3}-1}{(1-x)^{-2/3}-1}\right]^{\frac{11m+15}{4(m+3)}} \frac{d\eta}{(1-x\eta)^{5/3}\eta^{3/2}} \tag{48}$$

$$I_2(0;m) = \frac{4}{9}\left(\frac{m+3}{m+1}\right) \tag{49}$$

and where $I_2(x;m)/I_2(0;m)$ has been evaluated and plotted in figure 3 for $m = 0$, 1.0, 2.0 and 5.0.

The above results can now be applied to the previously discussed multi-room enclosure fires of reference 1. In those enclosure configurations, radiant heating of most wall surfaces (i.e., outside the burn room) was likely to have played a minor role in smoke movement phenomena during the time frames of the experiments. Accordingly, values of δ under conditions of convective wall layer heating have been computed from eqs. (41) and (46). These are presented in table 2 along with the results of all previous example calculations. As can be seen, for the cases considered, the values of δ for the convection driven wall heating examples are never greater than 0.011, and the original, small δ determination of the significance of the wall effect continues to be relevant.

6. QUASISTEADINESS OF THE WALL FLOWS AND A MEASURE OF THE LIKELIHOOD OF THEIR PENETRATION

The validity of two tacitly assumed aspects of the wall flow will be studied in this section. The first has to do with the question of the time required to reach quasisteadiness relative to an assumed steady quiescent upper layer. Related to this, the second has to do with the expectation that the velocities of the wall flow are large enough to actually penetrate the dropping upper layer - lower layer interface.

6.1 The Quasisteady Flow Assumption

The time, t_s, for a wall flow to establish itself as a steady flow (subsequent to a step change in wall/ambient temperature, and from the leading edge of the boundary layer to a station, x) has been studied extensively in the literature. Reference 7 presents a review of this work, and, in terms of the present nomenclature, recommends the following estimate for t_s

$$t_s = 3(1 - \zeta_i)^2 H^2/(Gr^{1/2}\nu_\infty) \tag{50}$$

When the time required for the upper layer to grow to a given thickness and temperature is at least as large as the above t_s estimate, then there is good reason to expect that the quasisteady wall flow assumption is valid. This observation together with the previous results for the t^m enclosure fire environment finally leads to the following criterion:

With regard to the development of the wall flow in the upper layer during t^m enclosure fires, the assumption of quasisteadiness is justified when layer interface elevations, ζ_i, satisfy

$$\frac{1}{(1-\zeta_i)}\left(\frac{\zeta_i^{-2/3}-1}{0.140}\right)^{3/2} \geq 3\left(\frac{m+1}{1-\delta}\right)^{1/2}\left(\frac{3}{m+3}\right)^{3/2}\frac{HP}{AX_2} \tag{51}$$

The criterion is illustrated in the upper curve of Figure 4, and has been successfully used to test the validity of the quasisteady assumption in all previously described fire scenarios.

6.2 Wall Layer Penetration

During a fire scenario it is reasonable to expect that the wall flow will penetrate the interface when the characteristic velocity of the former, say u_{max} of eq. (10), at elevation Z_i is much larger than that of the latter, i.e., when

$$u_{max}(Z = Z_i) >> dZ_i/dt \tag{52}$$

To be definite, the following criterion is adopted:

At the upper layer - lower layer interface, penetration of the wall flow into the lower layer is expected if

$$u_{max}(Z = Z_i) \geq 5dZ_i/dt \tag{53}$$

Using the present nomenclature and the previous results for the t^m enclosure fire environment, finally leads to the following version of eq. (53)

$$\frac{1}{\zeta_i^{5/3}}\left(\frac{\zeta_i^{-2/3}-1}{0.140}\right)^{1/2} \geq 1.9\left(\frac{m+1}{1-\delta}\right)^{1/2}\left(\frac{3}{m+3}\right)^{1/2}\frac{HP}{AX_2} \tag{54}$$

The criterion is illustrated in the lower curve of Figure 4, and has been successfully used to test the validity of the penetration assumption in all previously described fire scenarios.

7. SUMMARY AND CONCLUSIONS

The results of this work point to the significance of buoyancy driven wall flows on the development of hazardous environments within enclosures containing practical growing fires. Such flows were seen to be important, for example, in fire scenarios involving relatively weak fires and/or plan views with relatively long peripheral dimensions. It would clearly be appropriate to formulate and carry out an experimental program for quantitative verification of these results. In any event it appears that the wall flow phenomenon must be accounted for in mathematical enclosure fire models that hope to estimate dynamic environments generally for the purpose of predicting the response of fire detectors and fire intervention hardware and the time of onset of conditions detrimental to life safety. In order to carry out such an accounting, further analytic and/or experimental research on various aspects of the basic buoyancy driven wall flow may be required, and should be pursued. However, until the results of such studies are available, it may be prudent to add wall flow algorithms to existing models on a more timely basis. Such algorithms would be based on the kinds of calculation, estimates and results which have been developed in the present work. For engineering purposes, such algorithms may prove to be adequate, indeed, optimum, even in the long term.

8. ACKNOWLEDGMENTS

This work was supported by the U.S. Department of Health and Human Services, and the Bureau of Mines and National Park Service of the U.S. Department of Interior.

9. REFERENCES

[1] Cooper, L. Y., Harkleroad, M., Quintiere, J., and Rinkinen, W., An Experimental Study of Upper Hot Layer Stratification in Full-Scale Multi-room Fire Scenarios, J. of Heat Transfer, Vol. 104, 1982.

[2] Mulholland, G., Handa, T., Sugawa, O., Yamamato, H., Smoke Filling in an Enclosure, paper 81-HT-8, presented at 20th Joint ASME/AIChE National Heat Transfer Conf., Milwaukee, 1981.

[3] Jaluria, Y., Buoyancy-Induced Wall Flow Due to Fire in a Room, to appear as NBSIR, National Bureau of Standards.

[4] Ostrach, S., Laminar Flows with Body Forces, sect. F of Theory of Laminar Flows, Moore, F. K., Ed., Princeton, 1964.

[5] Ostrach, S., An Analysis of Laminar Free-Convection Flow and Heat Transfer about a Plate Parallel to the Direction of the Generating Body Force. NACA Rept. 1111, 1953.

[6] Eckert, E. R. G. and Jackson, T. W., Analysis of Turbulent Free-Convection Boundary Layer on Flat Plate, NACA Tech. Note 2207, 1950.

[7] Ede, A. J., Advances in Free Convection, Advances in Heat Transfer, Vol. 4, Hartnett, J. P. and Irving, T. F., Eds., Academic, 1967.

[8] Zukoski, E. E., Kubota, T., Cetegen, B., Entrainment in Fire Plumes, Fire Safety Journal, Vol. 3, Nos. 2-4, 1981.

[9] Cooper, L. Y., A Mathematical Model for Estimating Available Safe Egress Time in Fires, Fire and Materials, Vol. 6, Nos. 3-4, 1982.

[10] Heskestad, G., Engineering Relations for Fire Plumes, to appear in Fire Safety J.

[11] Cooper, L.Y., Convective Heat Transfer to Ceilings Above Enclosure Fires, 19th Inter. Symp. on Comb., Haifa, 1982.

[12] Cooper, L. Y., Development of Hazardous Conditions in Enclosures with Growing Fires, to appear in Combustion Science and Tech.

[13] Carslaw, H. S. and Jaeger, J. C., Conduction of Heat in Solids, Oxford, 1959.

[14] Peacock, R. D. and Breese, J. N., Computer Fire Modeling for the Prediction of Flashover, Nat. Bur. Stand. NBSIR, 1982.

10. NOMENCLATURE

A	area of enclosure
C_i	concentration of product i
C_p	specific heat of air
Gr_x	Grashoff number, eq. (2)
Gr	Gr_x at $x = H - Z_i$
g	acceleration of gravity
H	ceiling-to-fire distance
$\bar{h}$	average heat transfer coefficient
I_1, I_2	integrals, eqs. (43) and (48)
K	kinematic momentum flux, eq. (8)
k	thermal conductivity of air
k_w	thermal conductivity of wall material
L_{THICK}	thermally thick wall thickness
L_{THIN}	thermally thin wall thickness
m	an exponent
$\dot{m}$	mass flux
n	an exponent, eqs. (13) and (16)
$\overline{Nu_x}$	average Nusselt number, eq. (4)
P	perimeter
Pr	Prantl number
Q	energy release rate of fire
Q_o	a characteristic value of Q
Q_o^*	dimensionless Q_o, eq. (12)
$\bar{q}''$	rate of heat transfer per unit area
T	absolute temperature
t, t^*	time from ignition

t_I	a time of interest
u	downward velocity in wall flow
X_1, X_2, ... X_6	dimensionless parameters, eqs. (25), (34), (38), (42), and (47)
x	distance below ceiling
y	distance from wall
Z	elevation above fire
α	a constant, eq. (16)
Γ	gamma function
δ	dimensionless temperature difference, eq. (15)
ε	dimensionless parameter, eq. (18)
ζ	Z/H
η	dummy variable
κ	thermal diffusivity of air
κ_w	thermal diffusivity of wall material
λ_r	fraction of Q lost by radiation
λ_c	fraction of Q transferred to enclosure surface
μ	viscosity
ν	kinematic viscosity, μ/ρ
τ	dimensionless time, eq. (19)
ϕ	dimensionless temperature, T/T_∞
ψ	Q/Q_o

Subscripts

C	convective
i	interface
L	lower layer
max	maximum

p	plume
R	radiant
u	upper layer
w	wall flow
∞	ambient

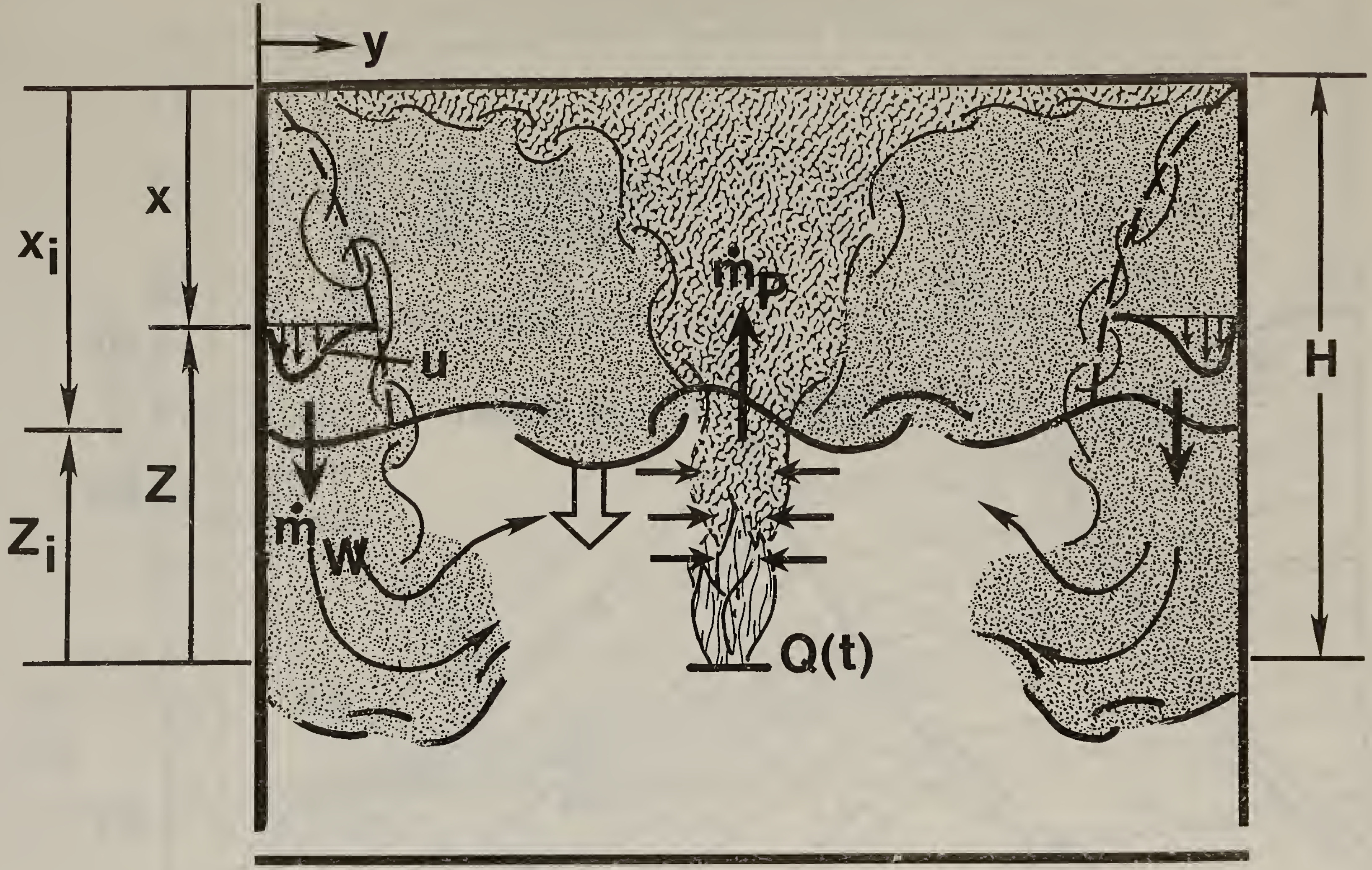

Figure 1. Sketch of the significant features of the wall effect

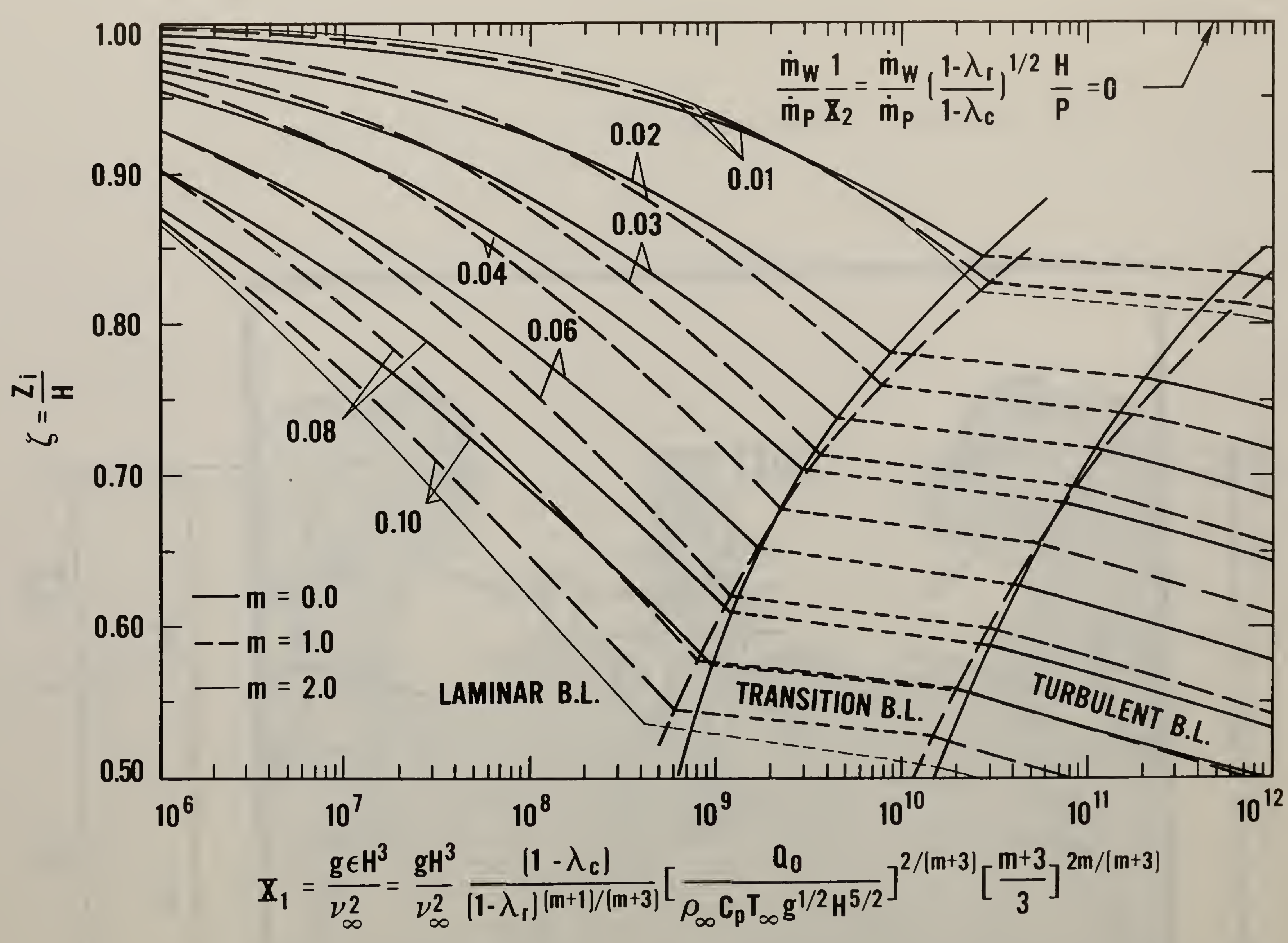

Figure 2. Plots of ζ_i as a function of X_1 per eqs. (23) and (24) for different values of $(\dot{m}_w/\dot{m}_p)/X_2$ and for $m = 0$, 1.0 and 2.0 under the assumption $\delta \ll 1$

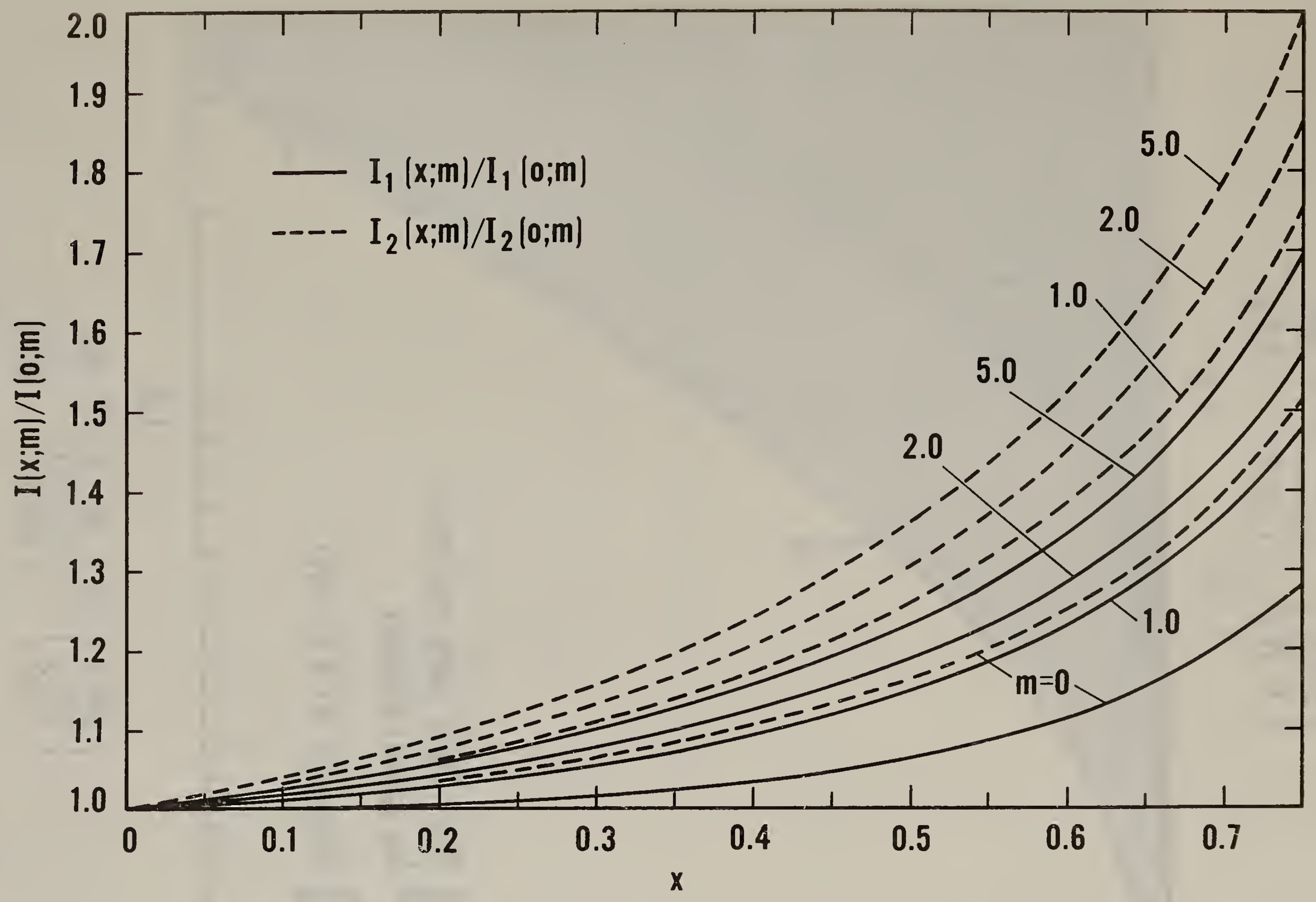

Figure 3. Plots of $I_1(x;m)/I_1(0;m)$ and $I_2(x;m)/I_2(0;m)$ per eqs. (43)-(44) and (48)-(49), respectively, for $m = 0$, 1.0, 2.0 and 5.0

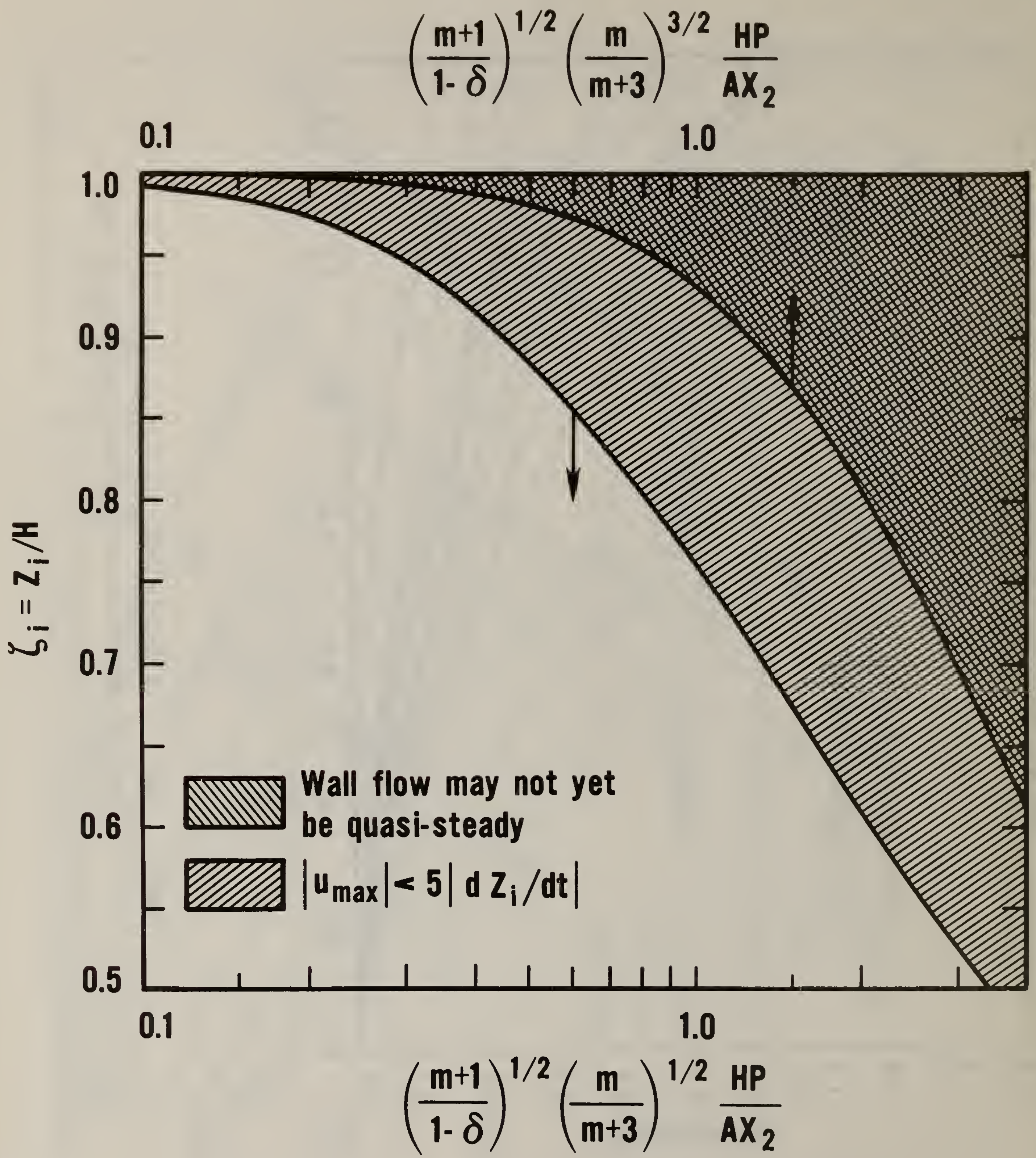

Figure 4. Plots of eq. (51) and (54) criteria for wall layer quasisteadiness and penetration, as functions of interface elevation and for t^m enclosure fires

Table 1. Thermal Conductivity and Diffusivity of Selected Materials

Material	Conductivity $k\left(\frac{W}{m^{o}K}\right)$	Diffusivity $\kappa\left(\frac{m^2}{s}\right)$
air[13]	0.024	$1.9(10^{-5})$
gypsum board[14]	0.17	$1.6(10^{-7})$
concrete (1:2:4)[11]	0.92	$4.2(10^{-7})$
steel (0.1% C)[11]	46.0	$1.2(10^{-5})$

Table 2. Results of Calculations on the Significance of the Wall Effect in Full-Scale Experiments of References 1 and 2

	λ_c	λ_r	ε	X_1	X_2	$\zeta_1 @ \frac{\dot{m}_w}{\dot{m}_p} = 0.3$	Wall Material	Wall Heating Condition	$\delta @ \frac{\dot{m}_w}{\dot{m}_p} = 0.3$
Mulholland et al.[2]									
16.2 kW, m = 0,	0.84	0.50	0.0036	$1.4(10^9)$	4.0	0.62	gyp. bd.	rad-thick:X_3 = 0.026	0.29
acetylene							concrete	rad-thick:X_3 = 0.0078	0.086
							1.5 mm steel	rad-thin:X_4 = 1.4	0.13
Cooper et al.[1]									
25 kW, m = 0,	0.87	0.19	0.0032	$1.3(10^9)$	15.	0.85	gyp. bd.	conv-thick:X_5 = 0.043	0.0093
89.6 m^2							concrete	conv-thick:X_5 = 0.013	0.0028
							1.5 mm steel	conv-thin:X_6 = 5.1	0.0082
225 kW, m = 0	0.75	0.24	0.027	$1.1(10^{10})$	12.	0.76	gyp. bd.	conv-thick:X_5 = 0.034	0.0081
40.6 m^2							concrete	conv-thick:X_5 = 0.010	0.0024
							1.5 mm steel	conv-thin:X_6 = 3.3	0.0043
ramp, m = 1,	0.81	0.24	0.0064	$2.6(10^9)$	39.	0.93	gyp. bd.	conv-thick:X_5 = 0.032	0.0059
40.6 m^2							concrete	conv-thick:X_5 = 0.010	0.0018
							1.5 mm steel	conv-thin:X_6 = 2.9	0.0024
ramp, m = 1,	0.71	0.24	0.0065	$2.7(10^9)$	27.	0.90	gyp. bd.	conv-thick:X_5 = 0.053	0.0110
89.6 m^2							concrete	conv-thick:X_5 = 0.016	0.0032
							1.5 mm steel	conv-thin:X_6 = 7.9	0.0081

NBS-114A (REV. 2-80)

U.S. DEPT. OF COMM. **BIBLIOGRAPHIC DATA SHEET** *(See instructions)*	1. PUBLICATION OR REPORT NO. NBSIR 83-2730	2. Performing Organ. Report No.	3. Publication Date June 1983

4. TITLE AND SUBTITLE

On the Significance of A Wall Effect in Enclosures with Growing Fires

5. AUTHOR(S)

Leonard Y. Cooper

6. PERFORMING ORGANIZATION *(If joint or other than NBS, see instructions)*

NATIONAL BUREAU OF STANDARDS
DEPARTMENT OF COMMERCE
WASHINGTON, D.C. 20234

7. Contract/Grant No.

8. Type of Report & Period Covered

9. SPONSORING ORGANIZATION NAME AND COMPLETE ADDRESS *(Street, City, State, ZIP)*

10. SUPPLEMENTARY NOTES

☐ Document describes a computer program; SF-185, FIPS Software Summary, is attached.

11. ABSTRACT *(A 200-word or less factual summary of most significant information. If document includes a significant bibliography or literature survey, mention it here)*

This paper studies the significance of a wall effect that has been observed during the growth stage of enclosure fire experiments. Relative to the two-layer phenomenon which tends to develop during such experiments, the effect has to do with the near-wall downward injection of hot upper layer gases into the relatively cool uncontaminated lower layer. It is conjectured that these observed wall flows are buoyancy driven, and that they develop because of the relatively cool temperatures of the upper wall whose surfaces are in contact with the hot upper layer gases. For a growing fire (growth proportional to t^m; t being time and $m \geq 0$) in an enclosed compartment, the conjectured mechanism for the wall flow leads to a time-dependent solution for the ratio of wall layer mass ejection rate from the upper layer, $\dot{m}_w$, to the fire plume mass injection rate to the upper layer, $\dot{m}_p$. The solution indicates that in practical fire scenarios $\dot{m}_w/\dot{m}_p$ can be of the order of "several tenths" even prior to the time that the upper layer interface has dropped to an elevation midway between the ceiling and fire. In other words, the results of the analysis indicate the importance of taking the wall effect into account in two-layer zonal analyses of enclosure fire phenomena.

12. KEY WORDS *(Six to twelve entries; alphabetical order; capitalize only proper names; and separate key words by semicolons)*

compartment fires, enclosure fires, fire growth, growing fires, mathematical modeling, smoke movement, two-layer phenomenon, wall flows.

13. AVAILABILITY

[X] Unlimited
☐ For Official Distribution. Do Not Release to NTIS
☐ Order From Superintendent of Documents, U.S. Government Printing Office, Washington, D.C. 20402.
[X] Order From National Technical Information Service (NTIS), Springfield, VA. 22161

14. NO. OF PRINTED PAGES

41

15. Price

$8.50

USCOMM-DC 6043-P80